LUND UNIVERSITY

Statistical signal analysis for the inverse source problem of electromagnetics

Nordebo, Sven; Gustafsson, Mats

2005

[Link to publication](#)

Total number of authors:
2

Statistical Signal Analysis for the Inverse Source Problem of Electromagnetics

Sven Nordebo and Mats Gustafsson

Sven Nordebo
Sven.Nordebo@msi.vxu.se

School of Mathematics and Systems Engineering
Växjö University
351 95 Växjö
Sweden

Mats Gustafsson
Mats.Gustafsson@es.lth.se

Department of Electroscience
Electromagnetic Theory
Lund Institute of Technology
P.O. Box 118
SE-221 00 Lund
Sweden

Abstract

A statistical signal analysis for the inverse source problem of electromagnetics is given. We consider the problem of estimating either the near field or the radiating current distribution from a measurement of the far field. The solution is derived via a linear operator formalism, and the ill-posedness of the reconstruction is quantified by using the Cramer-Rao lower bound which is explicitly given in terms of the multipole expansion of the electromagnetic field. A numerical study is included to illustrate the theoretical results.

1 Introduction

In this paper we demonstrate that the combination of electromagnetic theory, antenna theory and statistical signal processing yields simple and very useful tools for analyzing and quantifying the ill-posedness of the inverse source problem of electromagnetics. In particular, we derive the Cramer-Rao lower bound for estimating either the near field or the radiating current distribution from a measurement of the far field. From an engineering point of view, these inverse problems are important in the design and validation of high-performance radar antennas, radomes etc, see e.g. [11–13, 15, 19, 20].

The classical theory of radiating Q uses spherical vector modes (or multipoles) and equivalent circuits to analyze the properties of a hypothetical antenna inside a sphere, c.f. [2, 4, 7]. Hence, by considering an antenna of a given size and bandwidth, together with the Q-values which are computable for each mode, the maximum useful multipole order can be estimated by using the Fano broadband matching theory, see e.g. [5, 6, 17, 18]. From a radiating point of view, the high-order vector modes give the high-resolution aspects of the radiation pattern. As is well known, any attempt to accomplish supergain will result in high currents and near fields, thereby setting a practical limit to the gain available from an antenna of a given size, see also [9].

In [11], the minimum L^2 (minimum energy) solution to the inverse source problem is given for the full vector case where the source is a time harmonic three-dimensional current distribution confined within a sphere. The solution is derived via a linear operator formalism and is explicitly given in terms of the multipole expansion of the electromagnetic field [1, 8, 16]. In [12], the minimum energy solution is revived and extended to include a reactive power constraint using a Lagrangian formulation which can be optimized even more compactly using variational principles. In a measurement situation, the solution can be obtained by using the pseudoinverse, and the ill-posedness of the inverse problem is manifested by the exponential decay of the singular values for large mode orders. Thus, in practice, one can only reconstruct the low-order multipole components of the minimum energy representation of the source. In this paper, the ill-posedness and hence the resolution capabilities of the reconstruction given in [11] is quantified by using the Cramer-Rao lower bound which is explicitly given in terms of the multipole expansion of the electromagnetic field. The pseudoinverse as described in [11] does not necessarily exist when dealing with noisy data, and regularization theory is proposed as a remedy to this situation.

In our formulation, the regularization is obtained by setting a constraint on the maximum mode order, and hence the pseudoinverse does always exist. Furthermore, this is to our knowledge the first explicit statistical signal analysis of the inverse source problem employing estimation theory and the Cramer-Rao lower bound. In our view, the analysis technique is general and could be employed for investigating the sensitivity of many inverse problems including e.g. the reactive power constrained minimum energy solution derived in [12].

The investigation covers the two cases of infinite and finite measurements and includes a numerical study to illustrate the theoretical results.

2 The Cramer-Rao Lower Bound for Near Field Estimation

Assume that all sources are contained inside a sphere of radius $r = a$, and let $k = \omega/c$ denote the wave number, $\omega = 2\pi f$ the angular frequency, $\mathrm{e}^{-\mathrm{i}\omega t}$ the time-convention, and c and η the speed of light and the wave impedance of free space, respectively. The transmitted electric and magnetic fields, $\boldsymbol{E}(\boldsymbol{r})$ and $\boldsymbol{H}(\boldsymbol{r})$, can then be expanded in *outgoing spherical vector waves* $\boldsymbol{u}_{\tau ml}(k\boldsymbol{r})$ for $r > a$ as [1, 8, 16]

$$\boldsymbol{E}(\boldsymbol{r}) \;=\; \sum_{l=1}^{\infty}\sum_{m=-l}^{l}\sum_{\tau=1}^{2} f_{\tau ml}\boldsymbol{u}_{\tau ml}(k\boldsymbol{r}) \tag{2.1}$$

$$\boldsymbol{H}(\boldsymbol{r}) \;=\; \frac{1}{\mathrm{i}\eta}\sum_{l=1}^{\infty}\sum_{m=-l}^{l}\sum_{\tau=1}^{2} f_{\tau ml}\boldsymbol{u}_{\bar{\tau} ml}(k\boldsymbol{r}) \tag{2.2}$$

where $f_{\tau ml}$ are the expansion coefficients or multipole moments and $\bar{\tau}$ denotes the complementary index. Here $\tau = 1$ ($\bar{\tau} = 2$) corresponds to a transversal electric (TE) wave and $\tau = 2$ ($\bar{\tau} = 1$) corresponds to a transversal magnetic (TM) wave. The other indices are $l = 1, 2, \ldots, \infty$ and $m = -l \ldots, l$ where l denotes the *order* of that mode.

The outgoing spherical vector waves are given by

$$\begin{aligned}
\boldsymbol{u}_{1ml}(k\boldsymbol{r}) &= \mathrm{h}_l^{(1)}(kr)\boldsymbol{A}_{1ml}(\hat{\boldsymbol{r}}) \\
\boldsymbol{u}_{2ml}(k\boldsymbol{r}) &= \frac{1}{k}\nabla \times \boldsymbol{u}_{1ml}(k\boldsymbol{r}) = \\
\frac{(kr\mathrm{h}_l^{(1)}(kr))'}{kr}&\boldsymbol{A}_{2ml}(\hat{\boldsymbol{r}}) + \sqrt{l(l+1)}\frac{\mathrm{h}_l^{(1)}(kr)}{kr}\boldsymbol{A}_{3ml}(\hat{\boldsymbol{r}})
\end{aligned} \tag{2.3}$$

where $\boldsymbol{A}_{\tau ml}(\hat{\boldsymbol{r}})$ are the *spherical vector harmonics* and $\mathrm{h}_l^{(1)}(x)$ the *spherical Hankel functions of the first kind*, see [1, 8, 16]. The spherical vector harmonics $\boldsymbol{A}_{\tau ml}(\hat{\boldsymbol{r}})$ are given by

$$\begin{aligned}
\boldsymbol{A}_{1ml}(\hat{\boldsymbol{r}}) &= \frac{1}{\sqrt{l(l+1)}}\nabla \times (\boldsymbol{r}\mathrm{Y}_{ml}(\hat{\boldsymbol{r}})) \\
\boldsymbol{A}_{2ml}(\hat{\boldsymbol{r}}) &= \hat{\boldsymbol{r}} \times \boldsymbol{A}_{1ml}(\hat{\boldsymbol{r}}) \\
\boldsymbol{A}_{3ml}(\hat{\boldsymbol{r}}) &= \hat{\boldsymbol{r}}\mathrm{Y}_{ml}(\hat{\boldsymbol{r}})
\end{aligned} \tag{2.4}$$

where $Y_{ml}(\hat{\boldsymbol{r}})$ are the scalar *spherical harmonics* given by

$$Y_{ml}(\theta, \phi) = (-1)^m \sqrt{\frac{2l+1}{4\pi}} \sqrt{\frac{(l-m)!}{(l+m)!}} P_l^m(\cos\theta) e^{im\phi} \tag{2.5}$$

and where $P_l^m(x)$ are the *associated Legendre functions* [1]. For negative m-indices, the scalar waves satisfies the symmetry $Y_{-m,l}(\hat{\boldsymbol{r}}) = (-1)^m Y_{ml}^*(\hat{\boldsymbol{r}})$, and hence

$$\boldsymbol{A}_{\tau,-m,l}(\hat{\boldsymbol{r}}) = (-1)^m \boldsymbol{A}_{\tau ml}^*(\hat{\boldsymbol{r}}). \tag{2.6}$$

It can be shown that in the *far field* when $r \to \infty$, the electric field is given by

$$\boldsymbol{E}(\boldsymbol{r}) = \frac{e^{ikr}}{kr} \boldsymbol{F}(\hat{\boldsymbol{r}}) \tag{2.7}$$

where $\boldsymbol{F}(\hat{\boldsymbol{r}})$ is the *far field amplitude* given by

$$\boldsymbol{F}(\hat{\boldsymbol{r}}) = \sum_{l=1}^{\infty} \sum_{m=-l}^{l} \sum_{\tau=1}^{2} i^{-l-2+\tau} f_{\tau ml} \boldsymbol{A}_{\tau ml}(\hat{\boldsymbol{r}}). \tag{2.8}$$

By the orthonormality of the spherical vector harmonics on the unit sphere, the multipoles are given by

$$f_{\tau ml} = i^{l+2-\tau} \int \boldsymbol{A}_{\tau ml}^*(\hat{\boldsymbol{r}}) \cdot \boldsymbol{F}(\hat{\boldsymbol{r}}) \, d\Omega. \tag{2.9}$$

Suppose now that the measured far field $\boldsymbol{F}^{\mathrm{m}}(\hat{\boldsymbol{r}})$ is impaired by additive noise

$$\boldsymbol{F}^{\mathrm{m}}(\hat{\boldsymbol{r}}) = \boldsymbol{F}(\hat{\boldsymbol{r}}) + \boldsymbol{N}(\hat{\boldsymbol{r}}) \tag{2.10}$$

where $\boldsymbol{N}(\hat{\boldsymbol{r}})$ is a spatially uncorrelated complex Gaussian random process [14] with zero mean and dyadic covariance function

$$\mathcal{E}\{\boldsymbol{N}(\hat{\boldsymbol{r}})\boldsymbol{N}^*(\hat{\boldsymbol{r}}')\} = \sigma_n^2 \delta(\hat{\boldsymbol{r}} - \hat{\boldsymbol{r}}') \mathbf{I} \tag{2.11}$$

where $\mathcal{E}\{\cdot\}$ denotes the expectation, σ_n^2 the variance, $\delta(\hat{\boldsymbol{r}})$ the impulse function on the unit sphere and $\mathbf{I}$ the identity dyad. From (2.9), the measured multipole moments are thus given by

$$f_{\tau ml}^{\mathrm{m}} = i^{l+2-\tau} \int \boldsymbol{A}_{\tau ml}^*(\hat{\boldsymbol{r}}) \cdot \boldsymbol{F}^{\mathrm{m}}(\hat{\boldsymbol{r}}) \, d\Omega = f_{\tau ml} + n_{\tau ml} \tag{2.12}$$

where the noise term is

$$n_{\tau ml} = i^{l+2-\tau} \int \boldsymbol{A}_{\tau ml}^*(\hat{\boldsymbol{r}}) \cdot \boldsymbol{N}(\hat{\boldsymbol{r}}) \, d\Omega \tag{2.13}$$

and the estimated electric field is given by

$$\boldsymbol{E}^{\mathrm{m}}(\boldsymbol{r}) = \sum_{l=1}^{\infty} \sum_{m=-l}^{l} \sum_{\tau=1}^{2} f_{\tau ml}^{\mathrm{m}} \boldsymbol{u}_{\tau ml}(k\boldsymbol{r}). \tag{2.14}$$

Using (2.11) and the orthonormality of the spherical vector harmonics, we see that the noise term $n_{\tau ml}$ is an uncorrelated zero mean complex Gaussian random sequence with covariance function

$$\mathcal{E}\left\{n_{\tau ml}^* n_{\tau'm'l'}\right\} = \sigma_n^2 \delta_{\tau\tau'}\delta_{mm'}\delta_{ll'}. \tag{2.15}$$

The Cramer-Rao lower bound [10] for estimating the multipole moments in (2.12) is given by

$$\mathcal{E}\left\{|f_{\tau ml}^{\mathrm{m}} - f_{\tau ml}|^2\right\} \geq \frac{\sigma_n^2}{2}. \tag{2.16}$$

Since $f_{\tau ml}^{\mathrm{m}}$ is an uncorrelated random sequence, we find that the variance of the estimated electric field is given by

$$\mathcal{E}\left\{|\boldsymbol{E}^{\mathrm{m}}(\boldsymbol{r}) - \boldsymbol{E}(\boldsymbol{r})|^2\right\} = \sum_{l=1}^{\infty}\sum_{m=-l}^{l}\sum_{\tau=1}^{2}\mathcal{E}\left\{|f_{\tau ml}^{\mathrm{m}} - f_{\tau ml}|^2\right\}|\boldsymbol{u}_{\tau ml}(k\boldsymbol{r})|^2 \tag{2.17}$$

and the Cramer-Rao lower bound (2.16) give us

$$\mathcal{E}\left\{|\boldsymbol{E}^{\mathrm{m}}(\boldsymbol{r}) - \boldsymbol{E}(\boldsymbol{r})|^2\right\} \geq \frac{\sigma_n^2}{2}\sum_{l=1}^{\infty}\sum_{m=-l}^{l}\sum_{\tau=1}^{2}|\boldsymbol{u}_{\tau ml}(k\boldsymbol{r})|^2 \tag{2.18}$$

for $r > a$.

In principle, the lower bound in (2.18) is infinite, a notion which is reflecting up on the fact that it is impossible to estimate the near field from a far field measurement. However, for all practical purposes the maximum useful order $l_{\max}$ is finite and can be estimated as follows. The classical theory of radiating Q uses spherical vector modes and equivalent circuits to analyze the properties of a hypothetical antenna inside a sphere, c.f. [2, 4, 7]. Hence, by considering an antenna of a given electrical size ka and fractional bandwidth B, together with the Q-values which are computable for each mode order l [4], we can estimate $l_{\max}$ by using the Fano broadband matching theory and the expression

$$|\Gamma_l| \geq \mathrm{e}^{-\frac{\pi}{Q_l}\frac{1-B^2/4}{B}} \tag{2.19}$$

where Γ_l is the optimum reflection coefficient for a particular mode, see e.g. [5, 6, 17, 18]. Suppose e.g. that we are only interested in the modes (τ, m, l) contributing to the far field with coefficients $|f_{\tau ml}|^2 \leq \varepsilon$. The maximum useful order $l_{\max}$ then satisfies

$$|f_{\tau ml}|^2 \leq (1 - |\Gamma_l|^2)P_{\mathrm{in}} \leq \varepsilon \tag{2.20}$$

where P_{in} is the (appropriately scaled) input power. We note also that the optimum directivity is given by [9]

$$D_{\mathrm{opt}} = \frac{l_{\max}(l_{\max} + 2)}{2}. \tag{2.21}$$

Hence, if we consider an estimation situation confined to the class of optimum antennas with directivity less then D_{opt}, this is another option of determining $l_{\max}$.

The corresponding Cramer-Rao lower bound for estimating the near field *modulo* the higher order terms $> l_{\max}$, is finally given by

$$
\begin{aligned}
\mathcal{E}\left\{|\boldsymbol{E}^{\mathrm{m}}(\boldsymbol{r}) - \boldsymbol{E}(\boldsymbol{r})|^2\right\} &\geq \frac{\sigma_n^2}{2} \sum_{l=1}^{l_{\max}} \sum_{m=-l}^{l} \sum_{\tau=1}^{2} |\boldsymbol{u}_{\tau ml}(k\boldsymbol{r})|^2 = \\
&= \frac{\sigma_n^2}{2} \sum_{l=1}^{l_{\max}} \frac{2l+1}{4\pi} \left(\left| \mathrm{h}_l^{(1)}(kr) \right|^2 + \left| \frac{(kr\mathrm{h}_l^{(1)}(kr))'}{kr} \right|^2 + l(l+1) \left| \frac{\mathrm{h}_l^{(1)}(kr)}{kr} \right|^2 \right)
\end{aligned}
\tag{2.22}
$$

for $r > a$, and where we have employed the addition theorem for vector spherical harmonics [1] to obtain the equality. It is noted that the right hand side of (2.22) is independent of the spherical angles (θ, ϕ) and the same inequality will thus apply to the error norm

$$
\mathcal{E}\left\{\|\boldsymbol{E}^{\mathrm{m}}(\boldsymbol{r}) - \boldsymbol{E}(\boldsymbol{r})\|^2\right\} = \mathcal{E}\left\{\frac{1}{4\pi} \int |\boldsymbol{E}^{\mathrm{m}}(\boldsymbol{r}) - \boldsymbol{E}(\boldsymbol{r})|^2 \, \mathrm{d}\Omega\right\}
\tag{2.23}
$$

where $\mathrm{d}\Omega$ is the differential solid angle and the integral is defined over a sphere of radius r.

Suppose now that we make a finite measurement of I points in the far field,

$$
\boldsymbol{F}^{\mathrm{m}}(\hat{\boldsymbol{r}}_i) = \boldsymbol{F}(\hat{\boldsymbol{r}}_i) + \boldsymbol{N}(\hat{\boldsymbol{r}}_i)
\tag{2.24}
$$

for $i = 1, \ldots, I$. The *Fisher Information Matrix* [10] for measuring the multipole moments in this situation is given by

$$
[\mathbf{I}]_{\tau ml, \tau'm'l'} = \frac{2}{\sigma_n^2} \sum_{i=1}^{I} \frac{\partial \boldsymbol{F}^*(\hat{\boldsymbol{r}}_i)}{\partial f_{\tau ml}} \cdot \frac{\partial \boldsymbol{F}(\hat{\boldsymbol{r}}_i)}{\partial f_{\tau'm'l'}} = \frac{2}{\sigma_n^2} \sum_{i=1}^{I} \boldsymbol{A}_{\tau ml}^*(\hat{\boldsymbol{r}}_i) \cdot \boldsymbol{A}_{\tau'm'l'}(\hat{\boldsymbol{r}}_i)
\tag{2.25}
$$

and the corresponding Cramer-Rao lower bound for estimating the near field modulo the higher order terms $> l_{\max}$, is finally given by

$$
\mathcal{E}\left\{|\boldsymbol{E}^{\mathrm{m}}(\boldsymbol{r}) - \boldsymbol{E}(\boldsymbol{r})|^2\right\} \geq \sum_{l=1}^{l_{\max}} \sum_{m=-l}^{l} \sum_{\tau=1}^{2} \sum_{l'=1}^{l_{\max}} \sum_{m'=-l'}^{l'} \sum_{\tau'=1}^{2} \varepsilon_{\tau ml, \tau'm'l'}(k\boldsymbol{r})
\tag{2.26}
$$

for $r > a$, where

$$
\varepsilon_{\tau ml, \tau'm'l'}(k\boldsymbol{r}) = [\mathbf{I}^{-1}]_{\tau ml, \tau'm'l'} \boldsymbol{u}_{\tau ml}^*(k\boldsymbol{r}) \cdot \boldsymbol{u}_{\tau'm'l'}(k\boldsymbol{r}).
\tag{2.27}
$$

3 The Cramer-Rao Lower Bound for Source Estimation

Next, we derive the Cramer-Rao lower bound for the inverse source problem of electromagnetics as described in [11]. A brief review of the results in [11] is first given in order to accommodate the notation to the present more compact formulation using spherical vector waves.

It is assumed that all sources are contained inside a sphere of radius $r = a$. It is further assumed that the corresponding current distribution $\boldsymbol{J}(\boldsymbol{r})$ is sufficiently regular and satisfies the following wave equation for the electric and magnetic fields

$$\left(\nabla^2 + k^2\right) \boldsymbol{E}(\boldsymbol{r}) = -\mathrm{i}\left(\omega\mu_0 \boldsymbol{J}(\boldsymbol{r}) + \frac{1}{\omega\varepsilon_0}\nabla\nabla \cdot \boldsymbol{J}(\boldsymbol{r})\right) \tag{3.1}$$

$$\left(\nabla^2 + k^2\right) \boldsymbol{H}(\boldsymbol{r}) = -\nabla \times \boldsymbol{J}(\boldsymbol{r}) \tag{3.2}$$

where ε_0 and μ_0 are the permittivity and permeability of free-space, respectively, and $k = \omega\sqrt{\mu_0\varepsilon_0}$ and $\eta = \sqrt{\mu_0/\varepsilon_0}$ the corresponding wave number and wave impedance, respectively. Now, the multipole moments generated by the current $\boldsymbol{J}(\boldsymbol{r})$ are given by

$$f_{\tau ml} = -k^2\eta \int \chi(\boldsymbol{r}')\boldsymbol{v}_{\tau ml}^*(k\boldsymbol{r}') \cdot \boldsymbol{J}(\boldsymbol{r}') \,\mathrm{d}v' \tag{3.3}$$

where $\chi(\boldsymbol{r}) = 1$ for $r \leq a$ and zero elsewhere, and $\boldsymbol{v}_{\tau ml}(\boldsymbol{r})$ are the *regular spherical vector waves* defined by

$$\boldsymbol{v}_{1ml}(k\boldsymbol{r}) = \mathrm{j}_l(kr)\boldsymbol{A}_{1ml}(\hat{\boldsymbol{r}}) \tag{3.4}$$

$$\boldsymbol{v}_{2ml}(k\boldsymbol{r}) = \frac{1}{k}\nabla \times \boldsymbol{v}_{1ml}(k\boldsymbol{r}) \tag{3.5}$$

where $\mathrm{j}_l(x)$ is the *spherical Bessel function* of order l, cf. [1, 3, 11].

Let $\boldsymbol{J}(\mathbf{r}) \in X$ where X is the Hilbert space of L^2 measurable vector functions confined within $r \leq a$, and equipped with the scalar product $\langle \boldsymbol{J}_1, \boldsymbol{J}_2 \rangle_X = \int \chi(\boldsymbol{r})\boldsymbol{J}_1^*(\boldsymbol{r}) \cdot \boldsymbol{J}_2(\boldsymbol{r}) \,\mathrm{d}v$ (volyme integral over $r \leq a$) where $\mathrm{d}v$ is the differential volyme element. Further, let $\boldsymbol{F}(\hat{\boldsymbol{r}}) \in Y$ where Y is a finite dimensional Hilbert space of L^2 measurable transverse vector functions with $\hat{\boldsymbol{r}} \cdot \boldsymbol{F}(\hat{\boldsymbol{r}}) = 0$, and equipped with the scalar product $\langle \boldsymbol{F}_1, \boldsymbol{F}_2 \rangle_Y = \int \boldsymbol{F}_1^*(\hat{\boldsymbol{r}}) \cdot \boldsymbol{F}_2(\hat{\boldsymbol{r}}) \,\mathrm{d}\Omega$ (surface integral over the unit sphere) where $\mathrm{d}\Omega$ is the differential solid angle. It is further assumed that the finite dimensional subspace Y is spanned by the orthonormal spherical vector harmonics $\boldsymbol{A}_{\tau ml}(\hat{\boldsymbol{r}})$ up to and including the order $l_{\max}$.

A linear dyadic operator $\mathcal{L} : X \to Y$ that maps the space X onto the space Y is obtained by combining (2.8) (using $l_{\max}$) and (3.3)

$$\left(\mathcal{L}\boldsymbol{J}(\boldsymbol{r})\right)(\hat{\boldsymbol{r}}) = -k^2\eta \sum_{l=1}^{l_{\max}} \sum_{m=-l}^{l} \sum_{\tau=1}^{2} \mathrm{i}^{-l-2+\tau}\boldsymbol{A}_{\tau ml}(\hat{\boldsymbol{r}}) \int \chi(\boldsymbol{r}')\boldsymbol{v}_{\tau ml}^*(k\boldsymbol{r}') \cdot \boldsymbol{J}(\boldsymbol{r}') \,\mathrm{d}v'. \tag{3.6}$$

It is noted that the current $\boldsymbol{J}(\mathbf{r})$ may contain terms that belong to the nullspace of the operator $\mathcal{L}$. In particular, if we write $\boldsymbol{v}_{2ml}(k\boldsymbol{r}) = a(r)\boldsymbol{A}_{2ml}(\hat{\boldsymbol{r}}) + b(r)\boldsymbol{A}_{3ml}(\hat{\boldsymbol{r}})$, then $\mathcal{L}\left\{-b(r)\boldsymbol{A}_{2ml}(\hat{\boldsymbol{r}}) + a(r)\boldsymbol{A}_{3ml}(\hat{\boldsymbol{r}})\right\} = 0$. Note that in the present formulation, the nullspace of $\mathcal{L}$ also contains the vector waves $\boldsymbol{v}_{\tau ml}(k\boldsymbol{r})$ for $\tau = 1, 2$ and $l > l_{\max}$.

The Hilbert adjoint operator $\mathcal{L}^\dagger$ is defined by $\langle \boldsymbol{F}, \mathcal{L}\boldsymbol{J} \rangle_Y = \langle \mathcal{L}^\dagger\boldsymbol{F}, \boldsymbol{J} \rangle_X$, and is obtained by using (2.8) (using $l_{\max}$) and (3.6) and the orthonormality of the spherical vector harmonics. The result is

$$\left(\mathcal{L}^\dagger\boldsymbol{F}(\hat{\boldsymbol{r}})\right)(\boldsymbol{r}) = -k^2\eta\chi(\boldsymbol{r}) \sum_{l=1}^{l_{\max}} \sum_{m=-l}^{l} \sum_{\tau=1}^{2} f_{\tau ml}\boldsymbol{v}_{\tau ml}(k\boldsymbol{r}) \tag{3.7}$$

where $f_{\tau ml}$ are the multipole moments corresponding to the far field amplitude $\boldsymbol{F}(\hat{\boldsymbol{r}})$.

The minimum norm solution to the operator equation $\mathcal{L}\boldsymbol{J}(\boldsymbol{r}) = \boldsymbol{F}(\hat{\boldsymbol{r}})$ is given by $\boldsymbol{J}^{\dagger}(\boldsymbol{r}) = \mathcal{L}^{\dagger}\left(\mathcal{L}\mathcal{L}^{\dagger}\right)^{-1}\boldsymbol{F}(\hat{\boldsymbol{r}})$. The inverse operator $\left(\mathcal{L}\mathcal{L}^{\dagger}\right)^{-1}$ is found by considering the relation $\mathcal{L}\mathcal{L}^{\dagger}\tilde{\boldsymbol{F}}(\hat{\boldsymbol{r}}) = \boldsymbol{F}(\hat{\boldsymbol{r}})$ where $\boldsymbol{F}(\hat{\boldsymbol{r}}) \in Y$ and $\tilde{\boldsymbol{F}}(\hat{\boldsymbol{r}}) \in Y$ with corresponding coefficients $f_{\tau ml}$ and $\tilde{f}_{\tau ml}$ defined as in (2.8). Hence, by using (3.6) and (3.7), it is found that the inverse operator $\left(\mathcal{L}\mathcal{L}^{\dagger}\right)^{-1}$ is represented by

$$\tilde{f}_{\tau ml} = \frac{1}{(k^2\eta)^2}\frac{f_{\tau ml}}{\sigma_{\tau ml}^2} \tag{3.8}$$

where the *singular values* $\sigma_{\tau ml}^2$ are given by

$$\sigma_{\tau ml}^2 = \int \chi(\boldsymbol{r})|\boldsymbol{v}_{\tau ml}(k\boldsymbol{r})|^2 \, \mathrm{d}v. \tag{3.9}$$

It should be noted that the singular values $\sigma_{\tau ml}^2$ can be explicitely calculated [11], and that they *do not* depend on the m-index and could thus be written $\sigma_{\tau ml}^2 = \sigma_{\tau l}^2$. The minimum norm solution is finally given by

$$\boldsymbol{J}^{\dagger}(\boldsymbol{r}) = \mathcal{L}^{\dagger}\tilde{\boldsymbol{F}}(\hat{\boldsymbol{r}}) = -\frac{1}{k^2\eta}\chi(\boldsymbol{r})\sum_{l=1}^{l_{\max}}\sum_{m=-l}^{l}\sum_{\tau=1}^{2}\frac{f_{\tau ml}}{\sigma_{\tau ml}^2}\boldsymbol{v}_{\tau ml}(k\boldsymbol{r}). \tag{3.10}$$

Suppose that $\boldsymbol{F}^{\mathrm{m}}(\hat{\boldsymbol{r}})$ is the measured far field amplitude as in (2.10). The pseudosolution to the operator equation

$$\mathcal{L}\boldsymbol{J}(\boldsymbol{r}) = \boldsymbol{F}^{\mathrm{m}}(\hat{\boldsymbol{r}}) \tag{3.11}$$

is then given by

$$\boldsymbol{J}^{+}(\boldsymbol{r}) = -\frac{1}{k^2\eta}\chi(\boldsymbol{r})\sum_{l=1}^{l_{\max}}\sum_{m=-l}^{l}\sum_{\tau=1}^{2}\frac{f_{\tau ml}^{\mathrm{m}}}{\sigma_{\tau ml}^2}\boldsymbol{v}_{\tau ml}(k\boldsymbol{r}) \tag{3.12}$$

where $f_{\tau ml}^{\mathrm{m}}$ is given by (2.12) and represents the projection of the measured far field amplitude $\boldsymbol{F}^{\mathrm{m}}(\hat{\boldsymbol{r}})$ onto the finite dimensional subspace Y. Treating $f_{\tau ml}^{\mathrm{m}}$ as a stochastic variable as above, we see that $\mathcal{E}\{\boldsymbol{J}^{+}(\boldsymbol{r})\} = \boldsymbol{J}^{\dagger}(\boldsymbol{r})$, and the variance of the estimation error is

$$\mathcal{E}\left\{\left|\boldsymbol{J}^{+}(\boldsymbol{r}) - \boldsymbol{J}^{\dagger}(\boldsymbol{r})\right|^2\right\} = \frac{1}{(k^2\eta)^2}\sum_{l=1}^{l_{\max}}\sum_{m=-l}^{l}\sum_{\tau=1}^{2}\frac{\mathcal{E}\left\{|f_{\tau ml}^{\mathrm{m}} - f_{\tau ml}|^2\right\}}{\sigma_{\tau ml}^4}\left|\boldsymbol{v}_{\tau ml}(k\boldsymbol{r})\right|^2 \tag{3.13}$$

for $r \le a$. Using the Cramer-Rao lower bound associated with the estimation of multipoles given in (2.16), we get the following Cramer-Rao lower bound for estimating $\boldsymbol{J}^{\dagger}(\boldsymbol{r})$

$$\mathcal{E}\left\{\left|\boldsymbol{J}^{+}(\boldsymbol{r}) - \boldsymbol{J}^{\dagger}(\boldsymbol{r})\right|^2\right\} \ge \frac{1}{(k^2\eta)^2}\frac{\sigma_n^2}{2}\sum_{l=1}^{l_{\max}}\sum_{m=-l}^{l}\sum_{\tau=1}^{2}\frac{1}{\sigma_{\tau ml}^4}\left|\boldsymbol{v}_{\tau ml}(k\boldsymbol{r})\right|^2 \tag{3.14}$$

for $r \leq a$. Note that the summation over m-index can be performed explicitly in the same manner as with (2.22) by using the addition theorem for the vector spherical harmonics [1]. The result is

$$
\mathcal{E}\left\{\left|\boldsymbol{J}^+(\boldsymbol{r}) - \boldsymbol{J}^\dagger(\boldsymbol{r})\right|^2\right\} \geq
$$
$$
\frac{1}{(k^2\eta)^2} \frac{\sigma_n^2}{2} \sum_{l=1}^{l_{\max}} \frac{2l+1}{4\pi} \left(\frac{1}{\sigma_{1l}^4} \left|\mathrm{j}_l(kr)\right|^2 + \frac{1}{\sigma_{2l}^4} \left|\frac{(kr\mathrm{j}_l(kr))'}{kr}\right|^2 + \frac{1}{\sigma_{2l}^4}l(l+1) \left|\frac{\mathrm{j}_l(kr)}{kr}\right|^2 \right).
$$
$$(3.15)$$

Again, since the right hand side of (3.15) depends only on r, this result is also valid for the norm $\mathcal{E}\left\{\|\boldsymbol{J}^+(\boldsymbol{r}) - \boldsymbol{J}^\dagger(\boldsymbol{r})\|^2\right\}$ defined as in (2.23).

In the case with finite measurements as in (2.24), the Fisher information for measuring the multipoles is given by (2.25) and the corresponding Cramer-Rao lower bound is finally given by

$$
\mathcal{E}\left\{\left|\boldsymbol{J}^+(\boldsymbol{r}) - \boldsymbol{J}^\dagger(\boldsymbol{r})\right|^2\right\} \geq \frac{1}{(k^2\eta)^2} \sum_{l=1}^{l_{\max}} \sum_{m=-l}^{l} \sum_{\tau=1}^{2} \sum_{l'=1}^{l_{\max}} \sum_{m'=-l'}^{l'} \sum_{\tau'=1}^{2} \frac{\varepsilon_{\tau ml, \tau'm'l'}(k\boldsymbol{r})}{\sigma_{\tau ml}^2 \sigma_{\tau'm'l'}^2} \quad (3.16)
$$

for $r \leq a$, where

$$
\varepsilon_{\tau ml, \tau'm'l'}(k\boldsymbol{r}) = [\mathbf{I}^{-1}]_{\tau ml, \tau'm'l'} \boldsymbol{v}_{\tau ml}^*(k\boldsymbol{r}) \cdot \boldsymbol{v}_{\tau'm'l'}(k\boldsymbol{r}). \quad (3.17)
$$

Note that the singular values $\sigma_{\tau ml}^2$ in the reconstruction formulas (3.10) and (3.12) decay exponentially fast for $l \gg ka$ confirming ill-posedness of the inverse problem [11]. To this end, the Cramer-Rao lower bounds of (3.14) and (3.16) can be used to explicitly quantify the corresponding estimation accuracy.

4   Numerical examples

A numerical study has been performed in order to illustrate how the Cramer-Rao lower bound can be used as a means of quantifying and investigating the ill-posedness of the reconstruction (3.12).

In the examples below we focus on the Cramer-Rao lower bound for measuring $\boldsymbol{J}^\dagger(\boldsymbol{r})$ given by (3.15) and repeated here as [1]

$$
\mathcal{E}\left\{\left|\boldsymbol{J}^+(\boldsymbol{r}) - \boldsymbol{J}^\dagger(\boldsymbol{r})\right|^2\right\} \geq \frac{\sigma_n^2 k^2}{2\eta^2} F_{\mathrm{a}}(ka, kr, l_{\max}) \quad (4.1)
$$

where $F_{\mathrm{a}}(ka, kr, l_{\max})$ is the *CRB-accuracy factor* given by

$$
F_{\mathrm{a}}(ka, kr, l_{\max}) =
$$
$$
\frac{1}{(ka)^6} \sum_{l=1}^{l_{\max}} \frac{2l+1}{4\pi} \left(\frac{1}{\tilde{\sigma}_{1l}^4} \left|\mathrm{j}_l(kr)\right|^2 + \frac{1}{\tilde{\sigma}_{2l}^4} \left|\frac{(kr\mathrm{j}_l(kr))'}{kr}\right|^2 + \frac{1}{\tilde{\sigma}_{2l}^4}l(l+1) \left|\frac{\mathrm{j}_l(kr)}{kr}\right|^2 \right). \quad (4.2)
$$

---

[1]Note that we have made no assumptions about the frequency dependence of the noise variance σ_n^2 which is present in the factor $\frac{\sigma_n^2 k^2}{2\eta^2}$.
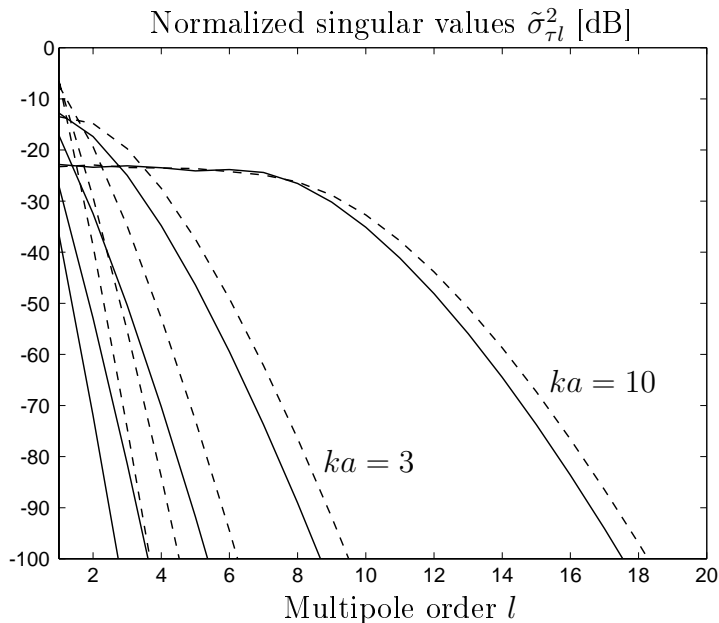
Figure 1: Normalized singular values $\tilde{\sigma}_{\tau l}^2$ as a function of multipole order l. Solid line is $\tilde{\sigma}_{1l}^2$ and dashed line is $\tilde{\sigma}_{2l}^2$. Electrical size is $ka = 0.1, 0.3, 1, 3, 10$.

Here, the *normalized singular values* $\tilde{\sigma}_{\tau l}^2$ are defined by $\sigma_{\tau l}^2 = a^3 \tilde{\sigma}_{\tau l}^2$ and calculated as

$$
\begin{aligned}
\tilde{\sigma}_{1l}^2 &= \frac{1}{2}\left(\mathrm{j}_l^2(ka) - \mathrm{j}_{l-1}(ka)\mathrm{j}_{l+1}(ka)\right) \\
\tilde{\sigma}_{2l}^2 &= \frac{1}{2l+1}\left((l+1)\tilde{\sigma}_{1,l-1}^2 + l\tilde{\sigma}_{1,l+1}^2\right)
\end{aligned}
\tag{4.3}
$$

following the derivation made in [11].

In Figure 1, the ill-posedness of the reconstruction is clearly displayed in view of the asymptotic exponential decay of the normalized singular values $\tilde{\sigma}_{\tau l}^2$. Figure 2 shows the corresponding CRB-accuracy factor $F_{\mathrm{a}}(ka, kr, l_{\max})$ as a function of maximum multipole order $l_{\max}$ when $r = a/2$ and for different electrical sizes ka. These plots clearly illustrate the difficulties of estimating the reconstruction as $l_{\max}$ increases and ka is small.

Figure 3 shows the CRB-accuracy factor $F_{\mathrm{a}}(ka, kr, l_{\max})$ as a function of relative radius r/a when $ka = 1$ and for different multipole orders $l_{\max}$. Again, the plot illustrates the difficulties of estimating the reconstruction as $l_{\max}$ increases. The plot further illustrates how the estimation performance improves closer to the center of the sphere. Even though this behaviour can be well explained from the expression (4.2) as $kr \to 0$, the result may first seem odd from a physical point of view. However, remembering that our investigation is restricted to the minimum norm solution $\boldsymbol{J}^\dagger$ *modulo* the higher order modes $l > l_{\max}$, it is clear that the estimation performance as $kr \to 0$ will tend to the optimum variance of estimating only the first order modes with $l = 1$.
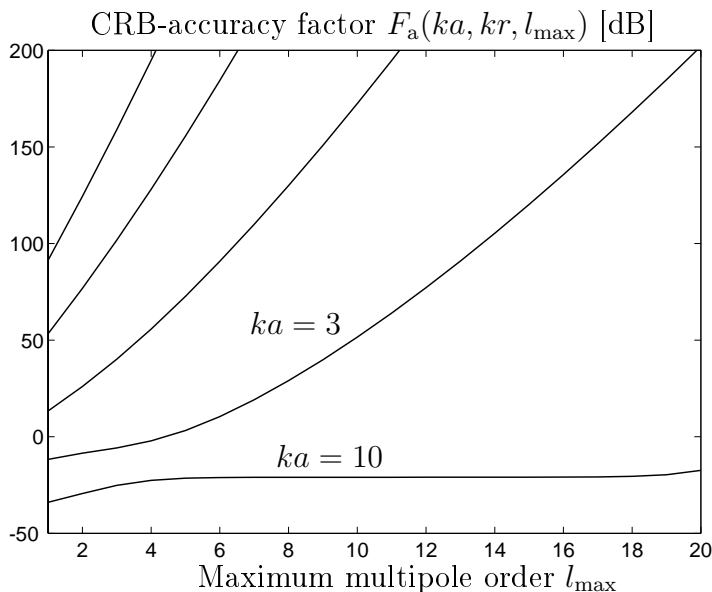
Figure 2: CRB-accuracy factor $F_a(ka, kr, l_{\max})$ as a function of maximum multipole order $l_{\max}$. Here $r = a/2$ and $ka = 0.1, 0.3, 1, 3, 10$.

5   Conclusion and future work

Although imaging and inverse scattering problems have been thoroughly studied during the last century there is only a partial understanding of these complex problems. Most of the efforts have been placed on the development of efficient inversion algorithms and mathematical uniqueness results. In comparison, there are very few results and a limited knowledge about the information content in the inversion data.

In this paper we provide the Cramer-Rao lower bound for the inverse source problem of electromagnetics which was presented in [11, 12]. We consider the problem of estimating either the near field or the radiating current distribution from a measurement of the far field. The solution is derived via a linear operator formalism and is explicitly given in terms of the multipole expansion of the electromagnetic field. The ill-posedness and hence the resolution capabilities of the reconstruction is explicitly quantified by using the Cramer-Rao lower bound. In particular, only the low order multipole components can be employed if the data is not perfect.

Future research is focused on establishing and merging tools and methods from statistical signal processing such as the *Fisher information* to quantify the quality of data in inverse scattering problems. Using these tools, the objective is furthermore to analyze fundamental properties of the inverse scattering problems with respect to various parameters of the system setup and of the physical model itself. Finally, given an objective function based on the Fisher information measure, we will also exploit and develop new convex interior point optimization techniques for efficient optimization of the system parameters such as suitable measurement positions, frequency bands etc.
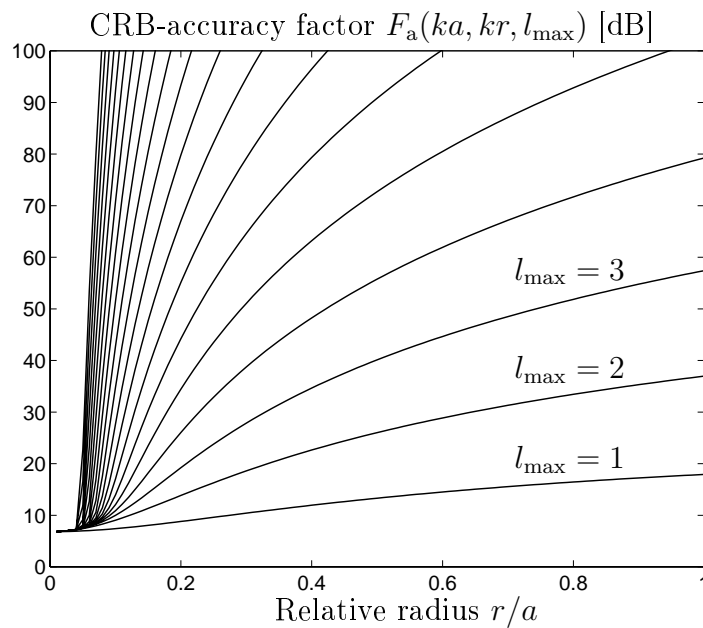
Figure 3: CRB-accuracy factor $F_{\mathrm{a}}(ka, kr, l_{\max})$ as a function of relative radius r/a. Here $ka = 1$ and maximum multipole order $l_{\max} = 1, \ldots, 20$.

References

[1] G. B. Arfken and H. J. Weber. *Mathematical Methods for Physicists*. Academic Press, New York, fifth edition, 2001.

[2] L. J. Chu. Physical limitations of Omni-Directional antennas. *Appl. Phys.*, **19**, 1163–1175, 1948.

[3] R. E. Collin. *Field Theory of Guided Waves*. IEEE Press, New York, second edition, 1991.

[4] R. E. Collin and S. Rothschild. Evaluation of antenna Q. *IEEE Trans. Antennas Propagat.*, **12**, 23–27, January 1964.

[5] R. M. Fano. Theoretical limitations on the broadband matching of arbitrary impedances. *Journal of the Franklin Institute*, **249**(1,2), 57–83 and 139–154, 1950.

[6] M. Gustafsson and S. Nordebo. On the spectral efficiency of a sphere. Technical Report LUTEDX/(TEAT-7127)/1–24/(2004), Lund Institute of Technology, Department of Electroscience, P.O. Box 118, S-211 00 Lund, Sweden, 2004. http://www.es.lth.se/teorel.

[7] R. C. Hansen. Fundamental limitations in antennas. *Proc. IEEE*, **69**(2), 170–182, 1981.

[8] J. D. Jackson. *Classical Electrodynamics*. John Wiley & Sons, New York, second edition, 1975.

[9] A. Karlsson. Physical limitations of antennas in a lossy medium. *IEEE Trans. Antennas Propagat.*, **52**, 2027–2033, 2004.

[10] S. M. Kay. *Fundamentals of Statistical Signal Processing, Estimation Theory.* Prentice-Hall, Inc., NJ, 1993.

[11] E. A. Marengo and A. J. Devaney. The inverse source problem of electromagnetics: Linear inversion formulation and minimum energy solution. *IEEE Trans. Antennas Propagat.*, **47**(2), 410–412, February 1999.

[12] E. A. Marengo, A. J. Devaney, and F. K. Gruber. Inverse source problem with reactive power constraint. *IEEE Trans. Antennas Propagat.*, **52**(6), 1586–1595, June 2004.

[13] E. A. Marengo and R. W. Ziolkowski. Nonradiating and minimum energy sources and their fields: Generalized source inversion theory and applications. *IEEE Trans. Antennas Propagat.*, **48**(10), 1553–1562, October 2000.

[14] K. S. Miller. *Complex Stochastic Processes.* Addison–Wesley Publishing Company, Inc., 1974.

[15] R. U. Nair and R. M. Jha. Tuning of EM performance for streamlined aircraft radomes. In *2004 IEEE Antennas and Propagation Society Symposium*, volume 1, pages 874–877. IEEE Antennas and Propagation Society, 2004.

[16] R. G. Newton. *Scattering Theory of Waves and Particles.* Dover Publications, New York, second edition, 2002.

[17] S. Nordebo and M. Gustafsson. Fundamental limitations for DOA estimation by a sphere. Technical Report LUTEDX/(TEAT-7128)/1–26/(2004), www.es.lth.se/teorel/, Lund Institute of Technology, Department of Electroscience, P.O. Box 118, S-211 00 Lund, Sweden, 2004.

[18] S. Nordebo and M. Gustafsson. Multichannel broadband Fano theory for arbitrary lossless antennas with applications in DOA estimation. In *2005 IEEE International Conference on Acoustics, Speech, and Signal Processing*, volume IV, pages 969–972, 2005.

[19] K. Persson and M. Gustafsson. Reconstruction of equivalent currents using a near-field data transformation – with radome applications. *Progress in Electromagnetics Research*, **54**, 179–198, 2005.

[20] A. D. Yaghjian. An overview of near-field antenna measurements. *IEEE Trans. Antennas Propagat.*, **34**(1), 30–45, January 1986.